# Ground-Based Radiometric Observations of Atmospheric Emission and Attenuation at 20.6, 31.65, and 90.0 GHz: A Comparison of Measurements and Theory

ED R. WESTWATER, JACK B. SNIDER, MEMBER, IEEE, AND MICHAEL J. FALLS

*Abstract*—**During 1987 and 1988, ground-based zenith-viewing observations of atmospheric thermal emission were made at frequencies of 20.6, 31.65, and 90.0 GHz. At the locations of the experiments—San Nicolas Island, CA, and Denver, CO—radiosonde observations of temperature and humidity were also available. Both National Weather Service and CLASS radiosondes were used in the study. The data, after conversion to attenuation by use of the mean radiating temperature approximation, were processed to derive attenuation statistics. Both clear and cloudy attenuation characteristics were examined and compared with results from recent theories. For the clear atmosphere, water vapor models of Waters and of Liebe were compared. At 20.6 and 31.65 GHz, the model of Waters agrees better with measurements; at 90.0 GHz, the model of Liebe is far superior. A recent model of Rosenkranz was used for oxygen absorption. For the average mass absorption coefficients for liquid clouds, measurement and theory generally agreed to within 30%. The predictability and interdependence of the three separate channels were also examined. It was found that attenuation for any two channels can predict that of the third to within 25%.**

## I. Introduction

OVER THE PAST DECADE, the Wave Propagation Laboratory (WPL) designed, constructed, and field tested several ground-based microwave radiometers [1], [2]. In particular, extensive experience has been gained by using both zenith-viewing and steerable dual-frequency instruments operating at 20.6 and 31.65 GHz. These instruments provide unique and meteorologically useful observations of precipitable water vapor $V$ and integrated cloud liquid $L$. Perhaps equally as useful, but certainly not as well studied, are the microwave attenuation characteristics that these devices can easily provide. For example, when simultaneous, colocated radiosondes are available, a well-calibrated radiometer can provide information for atmospheric absorption models. When radiosondes are not available, attenuation statistics and cloud information can still be derived.

In 1987, WPL added a channel at 90.0 GHz to the steerable and transportable radiometer. All three channels on this radiometer have equal beamwidths of 2.5°, and point in the same direction from the same location; hence, they are capable of simultaneously measuring emission and deriving attenuation for the same volume of air. We present here examples of some of the data taken with the new system at San Nicolas Island, CA, and at Denver, CO. From these data, several statistical and physical quantities, relevant to radio propagation studies, are derived and compared with theory.

Manuscript received March 31, 1989; revised April 26, 1990. This work was supported in part by the Office of Naval Research and by the Jet Propulsion Laboratories under the auspices of the National Aeronautics and Space Administration (NASA) as a part of the NASA Propagation program.

The authors are with National Oceanic and Atmospheric Administration/Environmental Research Laboratories, Wave Propagation Laboratory, Boulder, CO 80303-3328.

IEEE Log Number 9037631.

## II. Modeling of Microwave Radiative Transfer in the Atmosphere

### A. The Radiative Transfer Equation

In Sections V and VI, we compare brightness temperature measurements with calculations based on radiosonde observations. For completeness, we summarize here the equations and algorithms that are used in subsequent portions of the text. Since we are primarily concerned with ground-based observations of the troposphere obtained during nonprecipitating conditions, our analysis is based on the scalar radiative transfer equation that neglects scattering and polarization. Polarization effects are important for stratospheric and mesospheric observations in which Zeeman splitting, due to the Earth's magnetic field, is important, but may be neglected for tropospheric observations during nonprecipitating conditions. At the wavelengths of interest here, scattering is also negligible during nonprecipitating conditions.

The fundamental quantity describing atmospheric microwave radiation is the brightness temperature $T_b$ which depends on frequency, viewing angle, and polarization. For simplicity of notation, we suppress the dependence on these variables. For a nonscattering atmosphere in local thermodynamic equilibrium, $T_b$ is related to the absorptive and emissive properties of the medium by the radiative transfer equation [3], [4]

$$T_b = T_b^{\text{ext}} e^{-\tau(0,\infty)} + \int_0^\infty T(s)\alpha(s)e^{-\tau(0,s)}\,ds. \quad (1)$$

In (1), $T(s)$ is the absolute temperature, $s$ is the spatial

coordinate of an emitting volume, $\alpha(s)$ is the absorption coefficient, and $T_b^{\text{ext}}$ represents the radiation entering the atmosphere from external sources, such as radio stars, the sun, or the "big bang" cosmic background. The argument of the second exponential in (1) is called the optical depth $\tau(0, s)$

$$\tau(0, s) = \int_0^s \alpha(s')\, ds' \tag{2}$$

and $\tau(0, \infty)$ is called the opacity or total absorption. We use (1) and (2) to compute brightness temperatures and absorption from vertical distributions of temperature and absorption coefficient. Knowledge of the dependence of the absorption coefficient on meteorological variables allows one to calculate $T_b$ from radiosonde observations. However, since measurements of liquid are not routinely available from conventional radiosonde instruments, only measurements during clear conditions can be compared with calculations.

### B. Microwave Absorption

In the microwave region, the atmospheric absorption coefficient $\alpha$ is the sum of the separate contributions of gaseous $H_2O$ and $O_2$ and from clouds and rain. Absorption by trace constituents, such as $O_3$, is neglected here. Gaseous absorption is then a function of temperature $T$, pressure $P$, and water vapor density $\rho_v$, while cloud absorption depends primarily on $T$ and liquid water density $\rho_L$. We model atmospheric absorption as follows:

*Water Vapor Absorption:* Gaseous absorption by water vapor results from an electric dipole rotational transition at 22.235 GHz and the far wing contributions from strong infrared absorption lines. Two common models of water vapor absorption are the model of Waters [4] and the one of Liebe [5]. Liebe's model uses the known properties of all $H_2O$ spectral lines below 1000 GHz and the Van Vleck–Weisskopf line shape to calculate the absorption. In addition, a "continuum" term, which accounts for the influence of lines above 1000 GHz, as well as from possible dimer contributions, is added to the line contribution. This continuum was determined empirically from laboratory experiments. Waters' model uses the kinetic line shape model of Zhevakin–Naumov–Gross [6], [7] to fit the 22.235-GHz line and an empirical term to account for wing absorption. Waters' model is valid for frequencies below 100 GHz.

*Oxygen Absorption:* Oxygen absorption is due to a band of magnetic dipole rotational transitions centered at a frequency of 60 GHz. Because of the overlapping and interference of spectral lines at tropospheric pressures ($\sim$ 250 to 1000 mbar), a complex set of line intensities, line widths, and interference coefficients is necessary to describe the absorption. We use an updated version of $O_2$ interference coefficients given by [8]. Our experience has been that the wing absorption at 20.6, 31.65, and 90.0 GHz is sensitive to the values of the interference coefficients. For example, the constants of [9] gave rise to calculated brightness temperatures at 90.0 GHz that differed from our measurements (and from calculations based on the data of [8]) by about 5 K. However, $T_b$ values, calculated using the constants of [9], were in slightly better agreement with our meaurements at 20.6 and 31.65 GHz.

*Cloud Absorption:* Microwave absorption from liquid-bearing, but nonprecipitating, clouds depends primarily on the total amount of liquid present and does not depend on the size distribution of the liquid drops. To model cloud absorption, we use the Rayleigh approximation, as given by [10], together with the temperature and wavelength dependence of the dielectric constant of water, as given by [11].

### C. Weighting Functions

The radiative transfer equation (1) relates profiles of temperature and absorption coefficient to brightness temperature. In turn, by means of absorption models, profiles of absorption coefficient are related to profiles of $T$, $P$, $\rho_V$, and $\rho_L$. Since the dependence of absorption on meteorological variables is nonlinear, the dependence of brightness temperature on meteorological variables is nonlinear. However, to gain insight into how small changes in the meteorological profiles $\delta T(s)$, etc., give rise to small changes in brightness temperature $\delta T_b$, linearization is quite useful. In terms of small departures from an initial profile, linearization of (1) yields

$$\delta T_b = \int_0^\infty W_T(s)\delta T(s)\, ds + \int_0^\infty W_P(s)\delta P(s)\, ds + \int_0^\infty W_{\rho_V}(s)\delta\rho_V(s)\, ds + \int_0^\infty W_{\rho_L}(s)\delta\rho_L(s)\, ds \tag{3}$$

where $W_T(s)$ and $W_x(s)$ are the so-called weighting functions for $T$ and the generic variable $x$; $x$ is used to represent $P$, $\rho_V$, or $\rho_L$. Weighting functions for $T$ and $x$ are given by

$$W_T(s) = \alpha(s)e^{-\tau(0,s)} + e^{-\tau(0,s)}\frac{\partial\alpha(s)}{\partial T} \cdot \left[T(s) - T_b^{\text{ext}}e^{-\tau(s,\infty)} - \int_s^\infty T(s')\alpha(s')e^{-\tau(s,s')}\, ds'\right] \tag{4}$$

and

$$W_x(s) = e^{-\tau(0,s)}\frac{\partial\alpha(s)}{\partial x} \cdot \left[T(s) - T_b^{\text{ext}}e^{-\tau(s,\infty)} - \int_s^\infty T(s')\alpha(s')e^{-\tau(s,s')}\, ds'\right]. \tag{5}$$

For one not intimately familiar with weighting functions, a few words of explanation may be helpful. First consider $W_T$, whose units are $\text{km}^{-1}$. If we have a $\delta T$ (K) change in $T$ over a height interval $\delta h$ (km), the brightness temperature response $\delta T_b$ (K) to this change is $\overline{W}_T\, \delta T\, \delta h$, where $\overline{W}_T$ is the height average of $W_T$ over the interval $\delta h$. For water vapor, similar considerations lead to $\delta T_b$ (K) $= \overline{W}_{\rho_V}\delta\rho_V\delta h$. If the units of $\rho_V$ are $g \cdot \text{m}^{-3}$ and $h$ is in km, then their product $\delta V = \delta\rho_V \cdot \delta h$ has the units of mm. Thus $\delta T_b = \overline{W}_{\rho_V}\delta V$.

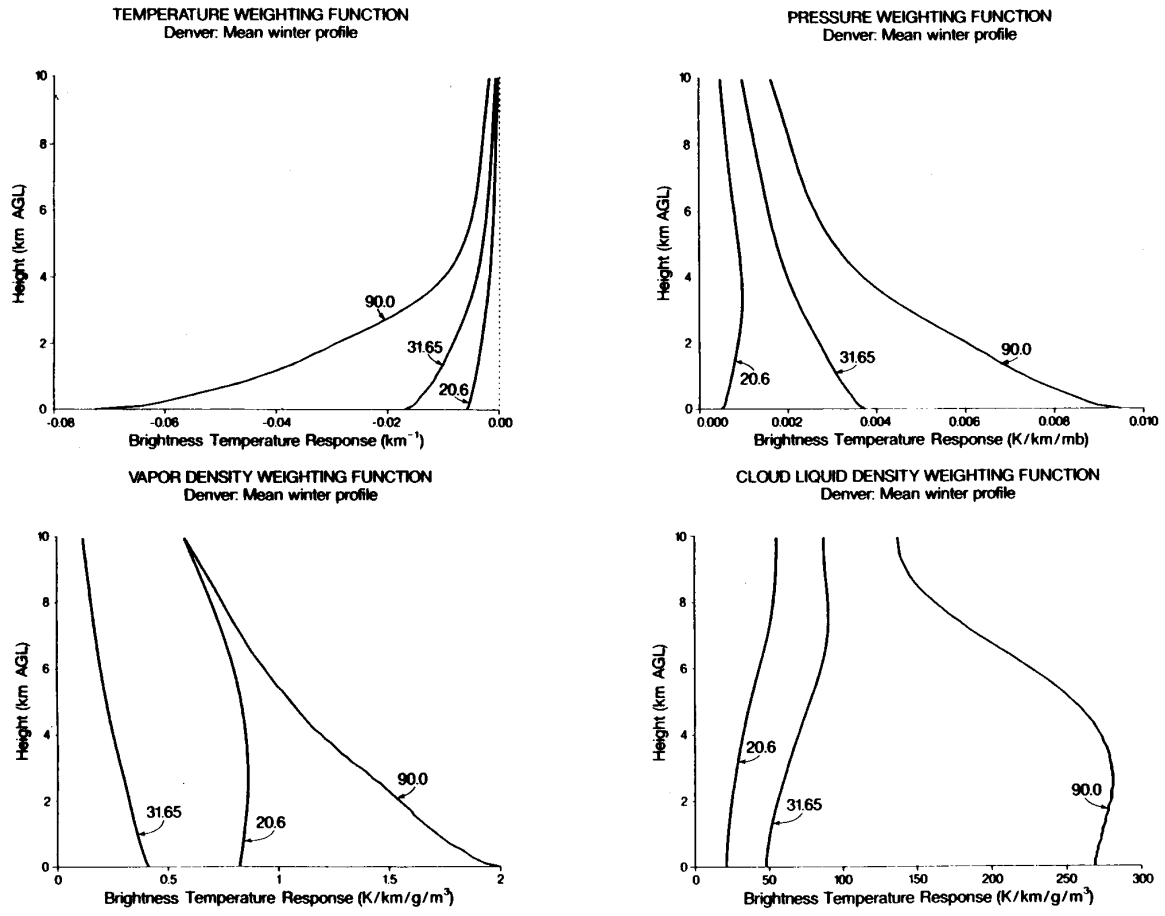


Fig. 1. Weighting functions for ground-based observations.

Plots of weighting functions, for zenith-viewing observations at 20.6, 31.65, and 90.0 GHz, are shown in Fig. 1 for the variables $T$, $P$, $\rho_V$, and $\rho_L$. For this figure, we used [5] for water vapor, [8] for oxygen, and [11] for cloud liquid. We note immediately that all three channels are quite insensitive to changes in $T$ or $P$. For example, referring to Fig. 1 for the temperature weighting function for 20.6 GHz, the average $W_T$ over the first kilometer is about $-0.005$ km$^{-1}$. Thus a change in temperature of 20 K over the first kilometer would lead to a $T_b$ change of $-0.1$ K. Relative to 20.6 and 31.65 channels, the channel at 90.0 GHz exhibits a stronger sensitivity to $\rho_V$ and a much stronger sensitivity to $\rho_L$. Finally, below about 5 km, both the vapor and cloud weighting functions at 20.6 and 31.65 GHz are nearly constant with height, which implies that variations in $T_b$ are primarily affected by variations in the column integrated amounts of vapor and liquid.

### *D. Mean Radiating Temperature Approximation*

The mean radiating temperature approximation is commonly used to derive attenuation from measurements of emission. With this approximation, (1) is written

$$T_b = T_b^{\text{ext}} e^{-\tau} + T_{mr}(1 - e^{-\tau}) \tag{6}$$

where $T_{mr}$ is the mean radiating temperature, and where we further simplify notation by replacing the total absorption $\tau(0, \infty)$ (in nepers) by $\tau$. Although $T_{mr}$ can be estimated from surface meteorological measurements, we estimate it from a monthly climatological average. As shown by the small temperature dependence of the weighting functions in Fig. 1, replacing the meteorologically varying profile $T(s)$ by a single constant is a good approximation at the frequencies of interest here. The accuracy of the approximation degrades for higher values of attenuation, and consequently, some caution is necessary for $T_b$ greater than, say, 150 K. Finally for our zenith-viewing observations, the cosmic background is such that $T_b^{\text{ext}} = 2.75$ K, and we frequently derive attenuation in decibels from $T_b$ by

$$\tau(\text{dB}) = 4.343 \ln \frac{T_{mr} - 2.75}{T_{mr} - T_b}. \tag{7}$$

## III. Description of Experiments

### *A. Motivation*

Field experiments were conducted with the transportable and steerable three-channel radiometer during 1987 and 1988. The locations of the experiments were San Nicolas Island, CA (SNI) and Denver, CO (DEN). The experiments were

designed to study the relative effects of vapor and liquid on the three channels, to gather attenuation statistics, and to determine the accuracy to which clear air brightness temperatures could be calculated from radiosonde observations.

### B. Radiometer Calibration

WPL radiometers are calibrated using the "tipping curve" method, in which the radiometer's antenna is scanned in elevation [12]. The purpose of calibration is to derive constants for use in a radiometer equation that relates measured internal system temperatures, reference temperatures, and output voltages to absolute brightness temperatures. The radiometers are continuously internally calibrated by comparing the response of two known internal reference temperatures to that of the antenna; the absolute calibration is to correct for system losses, detector constants, etc.

The basic measurements of the "tipping curve" method are, in addition to the previously mentioned internal measurements, the output voltage $v$ as a function of air mass $m$, where $m$ is equal to the secant of the zenith angle. The method assumes a stratified atmosphere which implies that absorption $\tau(m)$ at air mass $m$ is equal to $m$ times the zenith absorption $\tau(1)$. Measuring $\tau(m)$ for an adequate number (at least 3) and range (1 to 3 is good, 1 to 5 is better) of $m$'s allows two calibration constants to be determined. These constants relate input brightness temperature to radiometer output voltage. One equation of the method is derived by extrapolating the voltage $v(m)$ to $v(0)$. At $m = 0$, $\tau(0) = 0$, and $T_b = T_b^{\text{ext}} = 2.75$ K. The second constraint results from the requirement that $\tau(m)$ versus $m$ is a straight line. Because of the substantial spatial and temporal variation of cloud liquid water, tipping curves are performed only during clear sky conditions.

### C. Radiosonde Humidity Sensors

Different humidity sensors were employed by the radiosondes at SNI and DEN. Soundings at SNI were made using Vaisala RS80 radiosondes with HUMICAP humidity sensors. At DEN, soundings by the National Weather Service (NWS) used standard VIZ radiosondes with ACCU-LOK humidity sensors. We discuss the accuracy of NWS radiosondes in Section V. However, to the authors' knowledge, a rigorous intercomparison of the two units has not been made.

### D. San Nicolas Island, CA, July 1987

In July 1987, WPL participated in an investigation of the characteristics of marine stratocumulus clouds at (SNI), located approximately 50 nmi west of Los Angeles [13]. Zenith brightness temperatures at 20.6, 31.65, and 90.0 GHz. were observed continuously by the WPL radiometer. Although the primary purpose of the SNI observations was to study cloud properties, a secondary goal was to gather statistics on attenuation by cloud liquid water, especially at 90.0 GHz. Supporting data for the attenuation measurements at SNI were provided by radiosondes launched up to several times daily and by standard surface meteorological observations. Mean radiating temperatures were calculated from 69 radiosondes and the averages of these were used in the attenuation analysis.

Clouds with measurable liquid were persistent during the 3-week measurement period, being present 76% of the time. The amount of vapor $V$ was variable, ranging from 0.9 to 3.1 cm and having a mean value of 1.9 cm.

### E. Denver, CO, December 1987

The three-channel radiometer was installed at the Denver National Weather Service Forecast Office (NWSFO) in December 1987, where it operated next to the WPL six-channel radiometer (Microwave Radiometric Profiler, MRP), which measures $V$, $L$, and temperature profiles [1]. Supporting data were provided by the MRP, by the daily radiosondes released at standard times of 2300 and 1100 UTC, and by surface meteorological observations. $T_{mr}$ values for both December and August were calculated from 7 years of NWS radiosonde data.

Denver weather in December is characterized by relatively dry periods ($V \leq 0.5$ cm) and occasional periods of snow. Clouds containing supercooled liquid water are common, especially just before and during precipitation. In contrast to SNI, liquid-bearing clouds were present only 15% of the time. $V$ values were low, ranging from 0.1 to 1.0 cm and having a mean value of 0.5 cm.

### F. Denver, CO, August 1988

The three-channel radiometer was operated continuously during August 1988. These observations were taken under typical Denver summer conditions; the $V$ values were variable (1.06–3.29 cm with a mean value of 2.03 cm), and liquid-bearing clouds were present 11.8% of the time. As in December 1987, supporting data were provided by the MRP, by NWS radiosondes, and by surface meteorological observations.

### G. Denver, CO, GAPEX 1988

From October 29 to November 4, 1988, an intensive set of measurements was taken at Denver Stapleton Airport as a part of the Ground-based Atmospheric Profiling EXperiment (GAPEX). The objective of GAPEX was to acquire and analyze atmospheric temperature and moisture data from state-of-the art remote sensors [14]. Participants in the experiment included the Cooperative Institute for Meteorological Satellite Studies, the National Center for Atmospheric Research (NCAR), and the Wave Propagation Laboratory. Of particular interest is that meteorological observations were taken with two different types of radiosondes: those of the National Weather Service and those obtained from the NCAR-operated CLASS balloons. In all, we obtained 15 NWS soundings and 24 CLASS soundings during this period.

### H. Representative Time Series

Representative brightness temperatures measured simultaneously at each operating frequency are shown in Fig. 2 for SNI and DEN. The relative maxima and higher scintillation rates are associated with liquid-bearing clouds. Note the larger increases in brightness temperature at 90.0 GHz rela-

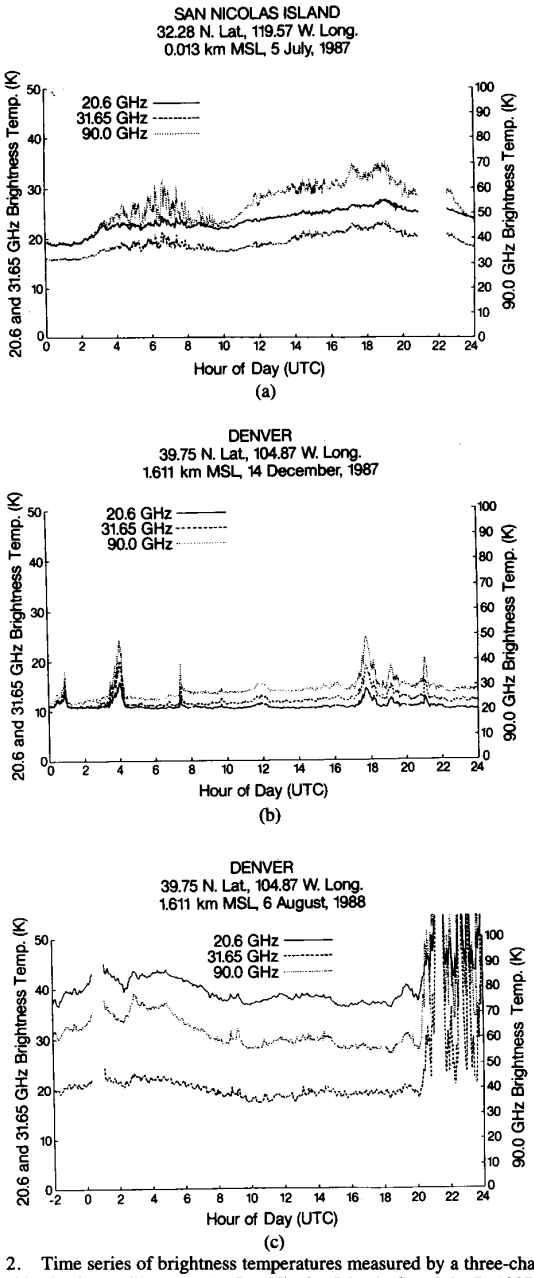


Fig. 2. Time series of brightness temperatures measured by a three-channel zenith-viewing radiometer. (a) San Nicolas Island, CA, July 5, 1987. (b) Denver, CO, December 14, 1987. (c) Denver, CO, August 6, 1988.

tive to 20.6 and 31.65 GHz as clouds pass through the radiometer antenna beam. Due to higher amounts of water vapor, brightness temperatures at all frequencies at DEN during August are higher than in December.

## IV. Attenuation Statistics

The data were edited in several ways before statistics were computed. First, 24-h time series of all data were plotted and then visually inspected for the presence of outliers or questionable points. For DEN data, measurements at 20.6 and 31.65 GHz were also available from an adjacent radiometer;

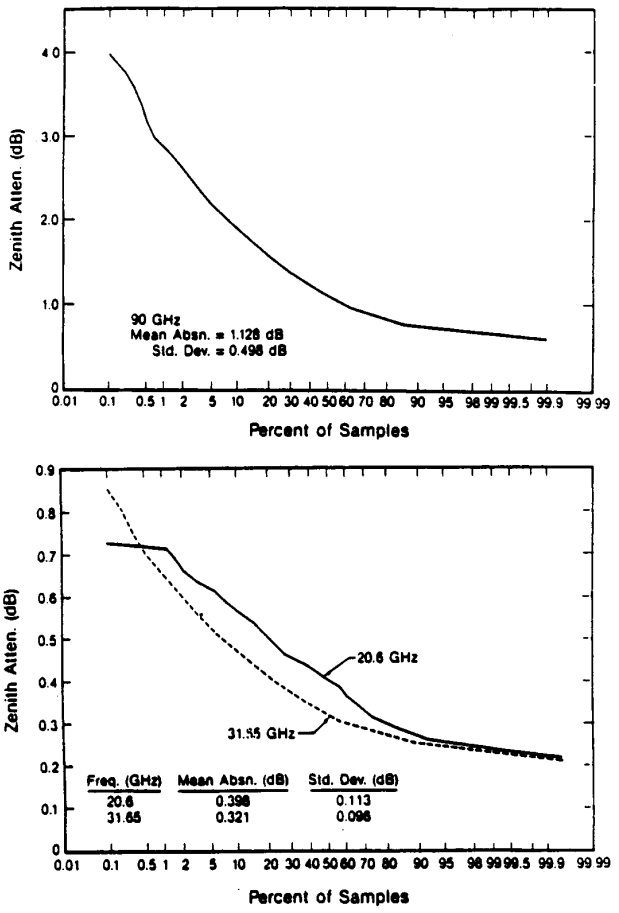


Fig. 3. Cumulative distribution of zenith attenuation measured by a three-channe l radiometer at San Nicolas Island, CA, July 1987. Data consist of 4805 5-min averages.

these also were used in visual editing. After the preliminary editing was completed, computer screening, based on approximately known physical relationships between the frequencies, was performed. This additional screening eliminated, for example, a segment of data in which snow on the antenna adversely affected the 90.0-GHz channel. After these stringent procedures were applied, there remained a total of 4805 5-min-average data for SNI (about 400 h), 14 181 2-min-average data for DEN December (about 473 h), and 17 792 2-min-average data for DEN August (about 598 h).

The cumulative distributions (Figs. 3–5) are markedly different for all three data sets and for all three frequencies. These differences reflect climatic differences between the two lcoations and between the two seasons at Denver: First, the sea-level altitude of SNI always results in dry attenuation greater than that at DEN. Second, the mean humidity at SNI and at DEN August are roughly a factor of three higher than at DEN December, resulting in a high absorption by vapor. The largest differences, however, were in cloud liquid: the marine stratocumulus clouds of SNI contained measurable liquid 76% of the time and were only rarely present at temperatures below 0.0°C; the winter clouds at DEN contained measurable liquid about 15% of the time and were

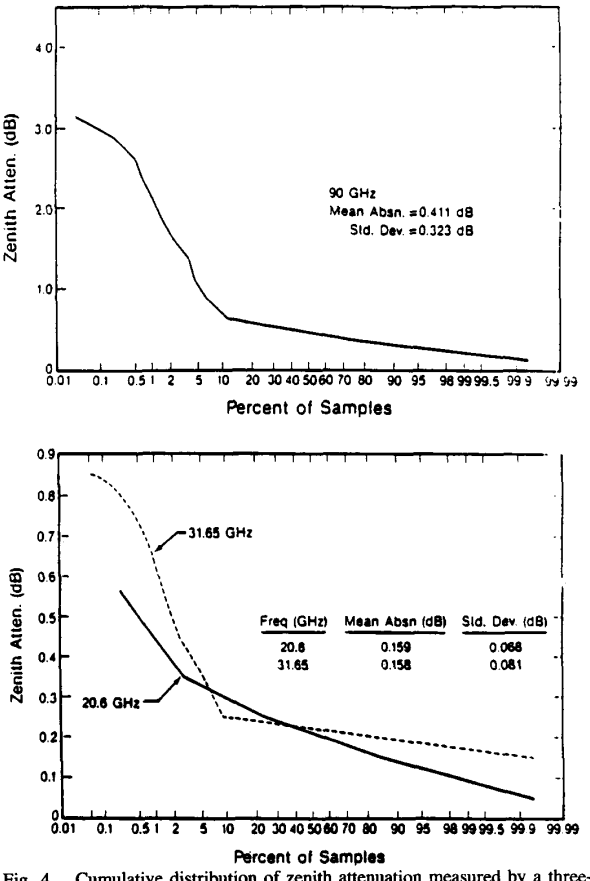


Fig. 4. Cumulative distribution of zenith attenuation measured by a three-channel radiometer at Denver, CO, December 1987. Data consist of 14 181 2-min averages.

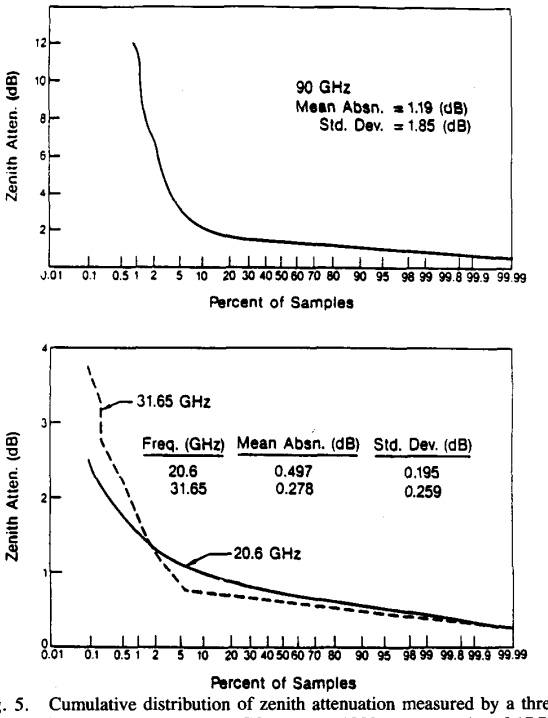


Fig. 5. Cumulative distribution of zenith attenuation measured by a three-channel radiometer at Denver, CO, August 1988. Data consist of 17 792 2-min averages.

frequently supercooled; the summer clouds at DEN were present roughly 12% of the time and, at times, contained much more liquid than those of SNI. Summer clouds in DEN frequently are cumulus and cumulonimbus types, both of which can contain large amounts of liquid.

Inspection of Figs. 3–5 reveals an important feature of the 20.6- and 31.65-GHz cumulative distributions; namely, that the two curves cross each other. For the highest values of attenuation, cloud liquid attenuation is the most important factor, and the 31-GHz attenuation is the larger of the two. For intermediate values, water vapor is the most important factor and 20-GHz attenuation is the larger. Finally, if the atmosphere is sufficiently dry, the 31-GHz attenuation will again exceed that of 20 GHz. These differences should be kept in mind when designing a 20/30-GHz communication system or when developing quality control procedures for 20/30-GHz radiometric data.

## V. Clear-Air Brightness Temperatures: Modeling Versus Experment

### A. Methodology

Measurements of temperature and humidity profiles together with multispectral emission measurements can provide useful informaton about absorption models. For example, using such data, different models can be compared, or, for a given model, model parameters can be derived. Here, we compare two models of water vapor absorption, namely those of [4 and [5]. The latest $O_2$ absorption model of [8] is assumed.

Equations (1) and (2) relate brightness temperature and optical depth to temperature and absorption along a given path. Since radiosonde soundings yield height profiles of temperature, pressure, and water vapor, height profiles of gaseous absorption coefficient $\alpha(h)$ can be calculated using models (see Section II). Thus for radiometric observations at zenith, measurements and calculations can be directly compared. Without a measurement of cloud liquid, only data taken under clear conditions could be compared.

The accuracy of the comparisons depends on a) the accuracy and representativeness of radiosonde data, and b) the absolute accuracy of the radiometer. Related to accuracy is the functional precisions of NWS radiosonde data [15] of $\pm 0.7$ mbar in pressure, $\pm 0.84°C$ in temperature, and $\pm 3.4°C$ in dewpoint temperature. The absolute accuracy of the WPL radiometer is estimated to be better than 1 K.

### B. Results

Comparisons of measurements and calculations were performed for each of the data sets of SNI (July 1987) and DEN (December 1987, and August, October–November 1988). The SNI observations and 24 of the Denver October–November ones were made with CLASS balloons; the remainder of the observations at DEN were made with NWS balloons.

TABLE I
COMPARISON OF MEASURED AND CALCULATED BRIGHTNESS TEMPERATURES FOR THE WATERS (W) AND LIEBE (L) ABSORPTION MODELS

| Frequency (GHz) | 20.6 | | 31.65 | | 90.0 | |
|---|---|---|---|---|---|---|
| Location | W | L | W | L | W | L |
| SNI | | | | | | |
| July (14 CLASS) | | | | | | |
| SLOPE | 0.97 | 0.88 | 0.96 | 0.87 | 1.22 | 0.91 |
| RMS (K) | 1.47 | 2.95 | 1.02 | 1.83 | 10.77 | 1.81 |
| DEN | | | | | | |
| Dec (22 NWS) | | | | | | |
| SLOPE | 0.94 | 0.85 | 0.98 | 0.86 | 1.33 | 0.96 |
| RMS (K) | 1.22 | 1.83 | 0.81 | 1.17 | 4.92 | 1.04 |
| Aug (37 NWS) | | | | | | |
| SLOPE | 0.95 | 0.88 | 0.89 | 0.90 | 1.13 | 1.03 |
| RMS (K) | 2.30 | 4.16 | 0.88 | 0.93 | 12.36 | 2.42 |
| Oct-Nov (15 NWS) | | | | | | |
| SLOPE | 0.90 | 0.81 | 0.78 | 0.70 | 1.25 | 0.90 |
| RMS (K) | 1.22 | 2.09 | 0.99 | 1.54 | 3.95 | 3.45 |
| Oct-Nov (24 CLASS) | | | | | | |
| SLOPE | 0.96 | 0.87 | 0.88 | 0.78 | 1.24 | 0.90 |
| RMS (K) | 0.70 | 1.53 | 0.75 | 1.26 | 5.33 | 2.14 |

Significant features of the comparisons are shown in Table I, in which slope (calculated/measured) and rms differences are shown. Several rather surprising features are seen from these comparisons. First, almost uniformly in all comparisons, the model of [4] has significantly less rms difference than that of [5] for the 20.6- and 31.65-GHz data. In addition, regression line slopes are generally closer to unity. The differences at 20.6 GHz, in particular, are due to modeling of the resonant line contributions. However, at 90 GHz, the situation is completely reversed, and the model of [5] is much more representative of the measured data. At the latter frequency, most of the contribution to the absorption comes from the continuum and/or nonresonant terms which are modeled completely differently by the two algorithms. Fig. 6 shows scatter plots, as well as other statistical quantities, for the entire data set.

The GAPEX data set gave us an opportunity to compare measurements with calculations based on two types of radiosondes. The NWS radiosondes were launched at 1100 and 2300 UTC; the CLASS radiosondes were launched about every 3 h for most of the experiment. The launch sites were about 10 m away from each other. Comparisons between simultaneous launches were only possible for four soundings, but a statistical comparison for the five-day period was possible (see Table II). We note that there is almost as much difference between brightness temperatures calculated from the two types of radiosondes as there is between brightness temperatures calculated for the two models. In addition, two possible outliers were found in the NWS data, both occurring on successive launches. One of the launches coincided with a CLASS launch, and the humidity data were perhaps 30% different. These particular soundings were dry, with the relative humidity frequently being less than 20%. As discussed in [16], such NWS data are suspect. In addition, CLASS observations generally offer a much greater number of reporting levels. For the GAPEX data set, the CLASS observations were generally in better agreement with observations than the NWS soundings. However, much more testing is required before general conclusions are made about which sensor is the more accurate.

## VI. MASS ABSORPTION COEFFICIENTS FOR WATER VAPOR

For clear conditions, there is an accurate and simple parameterization that relates zenith attenuation to integrated amounts of precipitable water vapor $V$.

$$\tau = \tau_{\text{dry}} + \kappa_V \cdot V \tag{8}$$

where

$$\kappa_V = \frac{1}{V}\int_0^\infty \alpha_V \, dh$$

and

$$\tau_{\text{dry}} = \int_0^\infty \alpha_{\text{dry}} \, dh.$$

In (8), the mass absorption coefficient $\kappa_V$ and the dry attenuation term $\tau_{\text{dry}}$ are related to the path integrals of the respective absorption coefficients for vapor $\alpha_V$ and for oxygen $\alpha_{\text{dry}}$. Due to profile variations of the relevant meteorological variables, the quantity $\kappa_V$ will also vary. However, for a given location and season, and at the frequencies of 20.6 and 31.65 GHz, calculations have shown that the variations in $\kappa_V$ are about 5% [17]. Using $V$ as a parameter, researchers [18] tried both a linear and a quadratic fit to their 3.3-mm (90.0-GHz) absorption data taken during clear conditions. There was no improvement over a linear fit by a quadratic. Thus we will use the linear form suggested by (8) as our parameterization, treating $\kappa_V$ and $\tau_{\text{dry}}$ as constants (to be determined) for each location and season. Since radiosonde humidity profiles can be integrated to derive $V$, the determination of effective $\tau_{\text{dry}}$ and $\kappa_V$ is straightforward; i.e., we determine regression coefficients $A$, $B$

$$\hat{\tau}_{\text{clr}} = A + BV. \tag{9}$$

The constants $A$ and $B$ that we derived from our data are shown in Table III. The data in these tables show excellent correlation between radiometrically determined absorption $\tau$ and radiosonde determined $V$, all correlation coefficients being greater than 0.93. Note also, that, as expected, dry coefficients $A$ increase with frequency, and also are greater at SNI, which is at sea level, than at DEN, which is 1.611 m ASL. Note also, for a given frequency, that there is at most a 15% variation in the mass absorption coefficients $B$, either for location or for season.

The values of 90-GHz attenuation given in Table III can also be compared with those of [18]. They reported $\hat{\tau}$ (dB) = $0.32 + 0.20V + 0.06V^2 \pm 0.18$ and $\hat{\tau}$ (dB) = $0.16 + 0.40V \pm 0.18$ as contrasted to our values $\hat{\tau}$ (dB) = $0.24 + 0.35V \pm 0.03$.

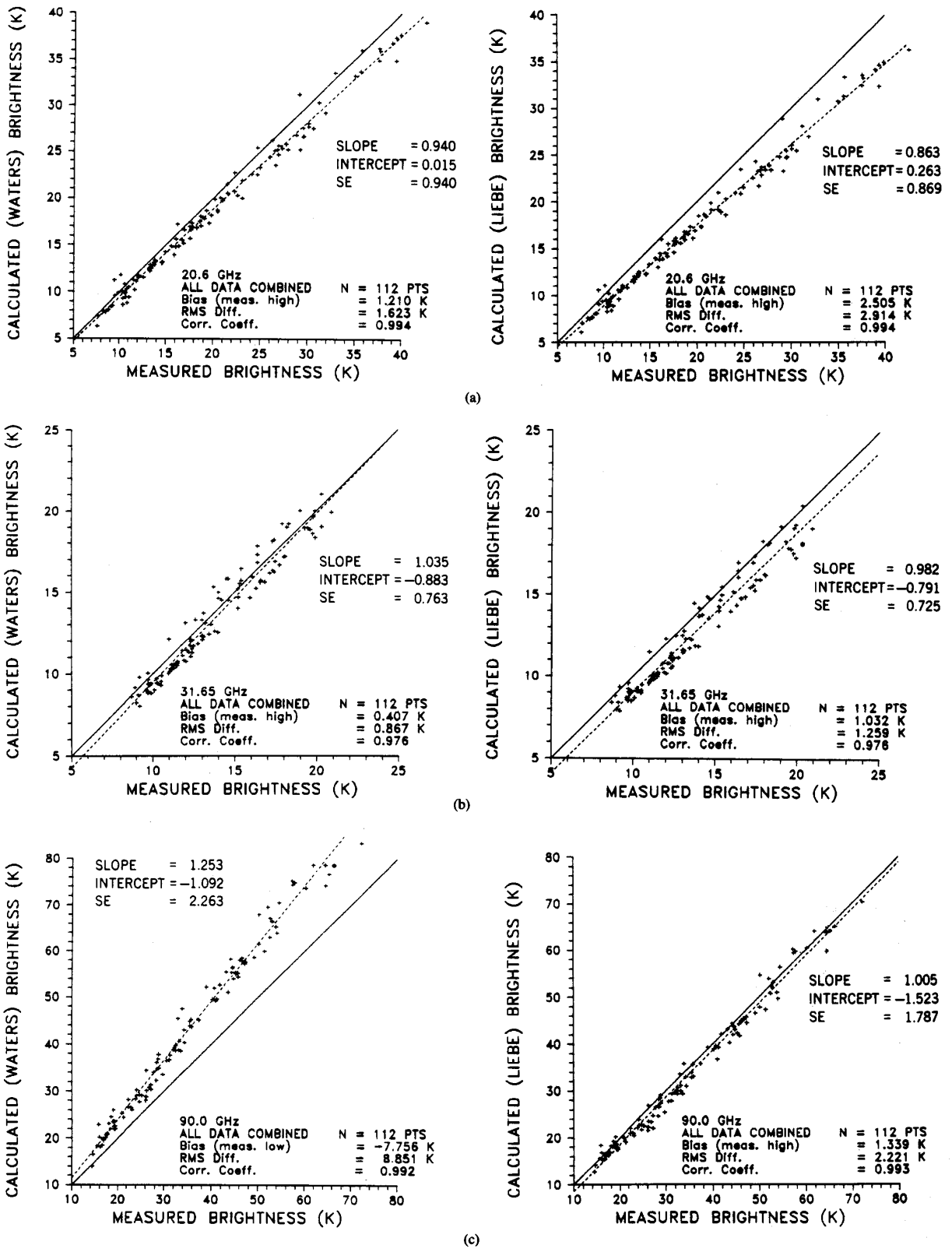


Fig. 6. Comparison of measured and calculated brightness temperatures at 20.6 (a), 31.65 (b), and 90.0 (c) GHz. Oxygen absorption calculated from the model of [8]. Solid line is 45°; dashed line is determined by regression.

TABLE II
GAPEX EXPERIMENT: COMPARISON OF NWS AND CLASS RADIOSONDES FOR CALCULATION OF BRIGHTNESS TEMPERATURES AT 20.6, 31.65, AND 90.0 GHz
SAMPLE SIZE OF NWS = 15; CLASS = 24

A: Waters Algorithm

| Radiosonde Type | NWS | CLASS | NWS | CLASS | NWS | CLASS |
|---|---|---|---|---|---|---|
| Frequency (GHz) | 20.6 | | 31.65 | | 90.0 | |
| BIAS (K) (meas.–calc.) | 1.15 | 0.53 | 0.96 | 0.88 | 3.78 | 5.00 |
| RMS (K) | 1.22 | 0.70 | 0.99 | 0.75 | 3.95 | 5.33 |
| Slope (calc./meas.) | 0.90 | 0.96 | 0.78 | 0.88 | 0.95 | 1.24 |
| Standard Error (K) | 0.39 | 0.46 | 0.39 | 0.29 | 0.94 | 1.22 |
| Corr. Coefficient | 0.98 | 0.99 | 0.97 | 0.98 | 0.97 | 0.99 |

B: Liebe Algorithm

| Radiosonde Type | NWS | CLASS | NWS | CLASS | NWS | CLASS |
|---|---|---|---|---|---|---|
| Frequency (GHz) | 20.6 | | 31.65 | | 90.0 | |
| BIAS (K) (meas.–calc.) | 2.03 | 1.41 | 1.51 | 1.20 | 3.31 | 1.85 |
| RMS (K) | 2.09 | 1.53 | 1.54 | 1.26 | 3.45 | 2.14 |
| Slope (calc./meas.) | 0.81 | 0.87 | 0.70 | 0.78 | 0.90 | 0.90 |
| Standard Error (K) | 0.34 | 0.87 | 0.15 | 0.26 | 1.27 | 0.95 |
| Corr. Coefficient | 0.98 | 0.99 | 0.97 | 0.98 | 0.95 | 0.99 |

TABLE III
REGRESSION COEFFICIENTS, DETERMINED FOR THREE FREQUENCIES, FOR PREDICTING CLEAR AIR ZENITH ABSORPTION $\tau$ (dB) FROM RADIOSONDE MEASUREMENTS OF PRECIPITABLE WATER VAPOR $V$ (cm) [SEE (9)]. $N$ = SAMPLE SIZE

Location: San Nicolas Island, California. July 1987. CLASS radiosondes.

| N = 14; V = 1.3 ± 0.29 cm | 20.6 GHz | 31.65 GHz | 90.0 GHz |
|---|---|---|---|
| A (dB) | 0.08 ± 0.01 | 0.14 ± 0.01 | 0.24 ± 0.04 |
| B (dB/cm) | 0.18 ± 0.01 | 0.08 ± 0.01 | 0.35 ± 0.03 |
| mean r (dB) | 0.32 ± 0.05 | 0.24 ± 0.02 | 0.72 ± 0.11 |
| std. err. est. r (dB) | 0.01 | 0.01 | 0.03 |
| (std. err./mean) × 100 | 3.4 | 2.9 | 4.4 |
| corr. coef. | 0.98 | 0.96 | 0.96 |

Location: Denver, Colorado. December 1987. NWS radiosondes.

| N = 22; V = 0.50 ± 0.28 cm | 20.6 GHz | 31.65 GHz | 90.0 GHz |
|---|---|---|---|
| A (dB) | 0.053 ± 0.005 | 0.097 ± 0.003 | 0.139 ± 0.008 |
| B (dB/cm) | 0.210 ± 0.008 | 0.075 ± 0.005 | 0.34 ± 0.01 |
| mean r (dB) | 0.16 ± 0.06 | 0.13 ± 0.02 | 0.31 ± .10 |
| std. err. est. r (dB) | 0.01 | 0.01 | 0.02 |
| (std. err./mean) × 100 | 6.9 | 4.5 | 5.8 |
| corr. coef. | 0.98 | 0.96 | 0.98 |

Location: Denver, Colorado. August 1987. NWS radiosondes.

| N = 37; V = 2.02 ± 0.52 cm | 20.6 GHz | 31.65 GHz | 90.0 GHz |
|---|---|---|---|
| A (dB) | 0.07 ± 0.02 | 0.07 ± 0.01 | 0.09 ± 0.04 |
| B (dB/cm) | 0.19 ± 0.01 | 0.075 ± 0.005 | 0.35 ± 0.02 |
| mean r (dB) | 0.46 ± .10 | 0.22 ± 0.04 | 0.81 ± 0.20 |
| std. err. est. r (dB) | 0.02 | 0.02 | 0.06 |
| (std. err./mean) × 100 | 5.2 | 7.2 | 8.1 |
| corr. coef. | 0.97 | 0.93 | 0.95 |

## VII. OBSERVATIONS OF ATTENUATION FROM CLOUDS

Calculations of microwave emission and attenuation from clouds are difficult to verify since conventional radiosondes do not measure cloud liquid. Even if they did, the highly variable temporal and spatial characteristics of clouds would make comparisons difficult. With our radiometer design of equal beamwidths at all three channels, emission from a common volume can be observed simultaneously. If we can estimate oxygen and water vapor emission when clouds are present, we can then study relative cloud effects between the three channels. Our procedure is straightforward but suffers from the defect that it derives cloud liquid $L$ and vapor $V$ from a dual-frequency algorithm that implicitly contains vapor and liquid absorption models. However, we believe that the interfrequency comparisons between 20.6 and 90.0 GHz and between 31.65 and 90.0 GHz are meaningful. In addition, the comparison between 20.6 and 31.65 is a check of consistency between measurements and theory; however, the comparison cannot be used for independent validation. The procedure we use is described as follows. We first establish a threshold $L_t$ for the presence of liquid-bearing clouds, using the 20.6- and 31.65-GHz channels. In the past, this threshold has proved to be effective in separating clear and cloudy conditions. Next, we derive $V$ from the dual-channel measurements. The retrieval coefficients used in deriving $V$ are semi-empirical and do not use the models of [4], [5]. However, this determination of $V$ has been extensively verified by comparison with radiosonde data, and indeed, is of the same order of accuracy as the radiosonde data. For data whose inferred $L$ is less than $L_t$, that is, the "clear" set, we derive a regression relation between the measured absorption $\tau_{\text{clr}}$ and $V$ as expressed by (9), again determining $A$ and $B$. Finally, for the data whose inferred $L$ is greater than $L_t$, that is, the "cloudy" set, we determine the cloud attenuation $\hat{\tau}_{\text{cld}}$ by

$$\begin{aligned}\hat{\tau}_{\text{cld}} &= \tau - \hat{\tau}_{\text{clr}} \\ &= \tau - A - B\hat{V} \\ &= C + D\hat{L}. \end{aligned} \tag{10}$$

The coefficient $D$ has the physical significance of the mass-absorption coefficient for cloud liquid, whereas if the procedure of subtracting clear attenuation from cloud attenuation were perfect, $C$ would be zero. It should be understood that $\hat{V}$ in (10) has been derived from the absorptions in cloudy conditions measured at 20.6 and 31.65 GHz. We also derive $\hat{L}$, but of course the accuracy of this determination has not been experimentally established, although theoretical estimates yield an accuracy of 0.0033 cm rms [19]. In Table IV we present the results of our regression analyses to determine $C$ and $D$. In addition, we show values of $D$ as derived from a regression analysis performed on cloud attenuations derived from cloud models inserted into an *a priori* data set of radiosondes for SNI and DEN.

The values presented in these tables show that there is agreement to within 35% of modeling and experiment. However, much more meaningful comparisons could be done if independent measurements of cloud liquid water were available.

## VIII. PREDICTABILITY OF ATTENUATION BETWEEN VARIOUS FREQUENCIES

A fairly extensive amount of brightness temperature data at 20.6 and 31.65 GHz is available. Since data at 90.0 GHz are

TABLE IV
REGRESSION COEFFICIENTS, DETERMINED FOR THREE FREQUENCIES, FOR PREDICTING THE ZENITH ABSORPTION FROM CLOUDS $\tau_{cld}$ (dB) FROM INTEGRATED CLOUD LIQUID $L$ (cm) [SEE (9) AND (10)]. $L \geq 0.0033$ CM, $N$ = SAMPLE SIZE

| Method | N | Coefficient | 20.6 GHz | 31.65 GHz | 90.0 GHz |
|---|---|---|---|---|---|
| Location: San Nicolas Island, July 1987 | | | | | |
| V, L from 2-$\nu$ radiometric retrievals | 14168 | C (dB) | 0.006 ± 0.002 | -0.007 ± 0.001 | 0.02 ± 0.01 |
| V, L from 2-$\nu$ radiometric retrievals | 14168 | D (dB/cm) | 3.56 ± 0.01 | 8.11 ± 0.01 | 45.23 ± 0.2 |
| L from cloud liquid model and radiosondes | 111 | D (dB/cm) | 2.63 ± 0.007 | 6.05 ± 0.01 | 39.63 ± 0.06 |
| Location: Denver, Colorado, December 1987 | | | | | |
| Method | N | Coefficient | 20.6 GHz | 31.65 GHz | 90.0 GHz |
| V, L from 2-$\nu$ radiometric retrievals | 2166 | C (dB) | -0.003 ± 0.001 | -0.007 ± 0.001 | 0.01 ± 0.005 |
| V, L from 2-$\nu$ radiometric retrievals | 2166 | D (dB/cm) | 4.26 ± 0.001 | 9.85 ± 0.002 | 36.8 ± 0.2 |
| L from cloud liquid model in *a priori* data base | 500 | D (dB/cm) | 4.5 ± 0.01 | 10.2 ± 0.002 | 52.98 ± 0.08 |
| Method | N | Coefficient | 20.6 GHz | 31.65 GHz | 90.0 GHz |
| Location: Denver, Colorado, August 1987 | | | | | |
| V, L from 2-$\nu$ radiometric retrievals | 2091 | C (dB) | 0.008 ± 0.0001 | 0.02 ± 0.0001 | 0.09 ± 0.02 |
| V, L from 2-$\nu$ radiometric retrievals | 2091 | D (dB/cm) | 3.67 ± 0.0003 | 8.45 ± 0.0003 | 38.4 ± 0.3 |
| L from cloud liquid model in *a priori* data base | 2217 | D (dB/cm) | 3.78 ± 0.01 | 8.49 ± 0.02 | 47.36 ± 0.07 |

not plentiful, and since simultaneous measurements at all three frequencies are scarce, it is of interest to examine their between-channel predictability. Such considerations are important when attenuation is being estimated at various locations, and also for multifrequency remote sensing, when the consideration of dependent channels is of utmost importance. We determined regression relations between the various channels for clear, cloudy, and all conditions. The form of the linear regression is

$$\tau(\text{dependent}) = c_0 + c_1\tau_1(\text{independent}) + c_2\tau_2(\text{independent}). \quad (11)$$

The results of the regression analyses are shown in Tables V–VII. It is clear from these tables that there is a high degree of predictability between the channels, and that if care is taken to distinguish between clear and cloudy conditions, the correlation coefficients are greater than about 0.90 for the linear regression equations. However, since the coefficients vary considerably from location to location, and, for a fixed location, from season to season, extrapolation between different climates is not suggested.

## IX. SUMMARY AND CONCLUSION

Measurements of atmospheric emission at 20.6, 31.65, and 90.0 GHz at climatically different locations and months (San Nicolas Island, CA, July 1987, and Denver, CO, December 1987 and August, October, November 1988) show reasonable consistency between theory and experiment, both in clear air and during cloudy conditions. For clear conditions, measurements were compared with calculations based on radiosonde data. A recent model of [8] was used for oxygen absorption, and two models, [4], [5], were used for water vapor. The model of [4] agreed better with measurements at 20.6 and 31.65 GHz, while the model of [5] was far superior at 90.0 GHz. This better agreement at 90.0 GHz probably was due to researchers in [5] having included more recent data into their nonresonant/continuum terms, especially laboratory data at 140 GHz. In addition, they explicitly accounted for all lines below 1000 GHz in their model. For a limited data set, we were able to compare measurements with calculations based on two types of radiosondes, the type operated by NWS and NCAR-operated CLASS radiosondes. The dif-

TABLE V
REGRESSION RELATIONS BETWEEN ABSORPTION $\tau$ (dB) AT 20.6, 31.65, AND 90.0 GHz AT SAN NICOLAS ISLAND, CA, JULY 1987 [SEE (11)]

| Regression relation | Statistics* | | |
|---|---|---|---|
| Clear conditions | | | |
| (L < 0.0025 cm; N = 3417) | | | |
| $\tau(20.6) = -0.271 - 0.055\,\tau(90.0) + 0.266\,\tau(31.65)$ | 0.011, | 0.986, | 3.5 |
| $\tau(31.65) = 0.086 + 0.141\,\tau(90.0) + 0.161\,\tau(20.6)$ | 0.003, | 0.995, | 1.1 |
| $\tau(90.0) = -0.332 - 0.107\,\tau(20.6) + 4.50\,\tau(31.65)$ | 0.015, | 0.991, | 2.2 |
| Cloudy conditions | | | |
| (L < 0.0025 cm; N = 14162) | | | |
| $\tau(20.6) = -0.044 - 0.890\,\tau(90.0) + 5.72\,\tau(31.65)$ | 0.041, | 0.933, | 6.3 |
| $\tau(31.65) = 0.093 + 0.172\,\tau(90.0) + 0.089\,\tau(20.6)$ | 0.005, | 0.999, | 1.4 |
| $\tau(90.0) = -0.539 - 0.460\,\tau(20.6) + 5.73\,\tau(31.65)$ | 0.029, | 0.998, | 2.1 |
| All data | | | |
| (N = 24129) | | | |
| $\tau(20.6) = -0.385 - 0.849\,\tau(90.0) + 5.43\,\tau(31.65)$ | 0.039, | 0.939, | 9.7 |
| $\tau(31.65) = 0.087 + 0.175\,\tau(90.0) + 0.092\,\tau(20.6)$ | 0.005, | 0.999, | 1.6 |
| $\tau(90.0) = -0.499 - 0.463\,\tau(20.6) + 5.64\,\tau(31.65)$ | 0.029, | 0.998, | 2.5 |

* Statistics are standard error of estimate, the correlation coefficient, and 100 times standard error of estimate divided by the mean.

TABLE VI
REGRESSION RELATIONS BETWEEN ABSORPTION $\tau$ (dB) AT 20.6, 31.65, AND 90.0 GHz AT DENVER, CO, DECEMBER 1987 [SEE (11)]

| Regression relation | Statistics* | | |
|---|---|---|---|
| Clear conditions | | | |
| (L < 0.0033 cm; N = 12105) | | | |
| $\tau(20.6) = -0.272 - 0.023\,\tau(90.0) + 3.57\,\tau(31.65)$ | 0.024, | 0.889, | 16.1 |
| $\tau(31.65) = 0.076 + 0.136\,\tau(90.0) + 0.108\,\tau(20.6)$ | 0.004, | 0.972, | 3.0 |
| $\tau(90.0) = -0.396 - 0.252\,\tau(20.6) + 5.57\,\tau(31.65)$ | 0.026, | 0.958, | 8.2 |
| Cloudy conditions | | | |
| (L < 0.0033 cm; N = 2166) | | | |
| $\tau(20.6) = 0.055 + 0.047\,\tau(90.0) + 0.443\,\tau(31.65)$ | 0.028, | 0.956, | 12.6 |
| $\tau(31.65) = 0.019 + 0.178\,\tau(90.0) + 0.455\,\tau(20.6)$ | 0.028, | 0.981, | 10.0 |
| $\tau(90.0) = -0.207 + 0.892\,\tau(20.6) + 3.27\,\tau(31.65)$ | 0.122, | 0.958, | 13.3 |
| All data | | | |
| (N = 14181) | | | |
| $\tau(20.6) = 0.084 + 0.139\,\tau(90.0) + 0.107\,\tau(31.65)$ | 0.040, | 0.802, | 25.2 |
| $\tau(31.65) = 0.056 + 0.242\,\tau(90.0) + 0.014\,\tau(20.6)$ | 0.014, | 0.984, | 9.0 |
| $\tau(90.0) = -0.229 + 0.279\,\tau(20.6) + 3.78\,\tau(31.65)$ | 0.056, | 0.985, | 13.7 |

* Statistics are as in Table V.

TABLE VII
REGRESSIO RELATIONS BETWEEN ABSORPTION $\tau$ (dB) AT 20.6, 31.65, AND 90.0 GHz AT DENVER, CO, AUGUST 1987 [SEE (11)]

| Regression relation | Statistics* | | |
|---|---|---|---|
| Clear conditions | | | |
| (L < 0.0033 cm; N = 15701) | | | |
| $\tau(20.6) = 0.039 + 0.451\,\tau(90.0) + 0.236\,\tau(31.65)$ | 0.027, | 0.968, | 6.1 |
| $\tau(31.65) = 0.056 + 0.177\,\tau(90.0) + 0.047\,\tau(20.6)$ | 0.012 | 0.961, | 5.6 |
| $\tau(90.0) = -0.148 + 0.072\,\tau(20.6) + 2.125\,\tau(31.65)$ | 0.043, | 0.978, | 5.3 |
| Cloudy conditions | | | |
| (L < 0.0033 cm; N = 2091; $\tau(90.0)$ < 12 dB) | | | |
| $\tau(20.6) = 0.046 + 0.024\,\tau(90.0) + 0.425\,\tau(31.65)$ | 0.067, | 0.961, | 8.3 |
| $\tau(31.65) = -0.404 + 0.090\,\tau(90.0) + 0.995\,\tau(20.6)$ | 0.103, | 0.972, | 15.5 |
| $\tau(90.0) = -0.141 + 0.119\,\tau(20.6) + 3.460\,\tau(31.65)$ | 0.637, | 0.954, | 22.1 |
| All data | | | |
| (N = 17792; $\tau(90.0)$ < 12 dB) | | | |
| $\tau(20.6) = 0.310 + 0.051\,\tau(90.0) + 0.487\,\tau(31.65)$ | 0.084, | 0.878, | 16.9 |
| $\tau(31.65) = 0.006 + 0.182\,\tau(90.0) + 0.151\,\tau(20.6)$ | 0.047, | 0.975, | 17.2 |
| $\tau(90.0) = -0.332 + 0.380\,\tau(20.6) + 4.347\,\tau(31.65)$ | 0.229, | 0.974, | 21.8 |

* Statistics are as in Table V.

ferences in calculated brightness temperatures based on the two types of radiosondes was as large as the differences between the two water vapor models. When all data were combined together, except for model [4] at 90.0 GHz, generally excellent agreement between measurements and calculations was obtained—the poorest correlation coefficient was 0.976. The determinations of cloudy attenuation values are reasonably consistent with theory, being within 35%. Probability distributions for attenuation were derived for the three climatologies and were both location- and season-dependent. Finally, we demonstrated that at a given location and season, the attenuations from any two of the channels could significantly predict the attenuation of the remaining one (correlation coefficients greater than 0.90). This predictability is based on stratifying the data sets into clear and cloudy samples and then using linear regression analysis.

## Acknowledgment

The authors wish to thank M. T. Decker, D. C. Hogg (NOAA/CIRES), and R. Hill (NOAA) for useful comments on the manuscript.

## References

[1] D. C. Hogg, M. T. Decker, F. O. Guiraud, K. B. Earnshaw, D. A. Merritt, K. P. Moran, W. B. Sweezy, R. G. Strauch, E. R. Westwater, and C. G. Little, "An automatic profiler for the temperature, wind, and humidity in the troposphere," *J. Appl. Meteorol.*, vol. 22, pp. 807-831, 1983.

[2] E. R. Westwater, and J. B. Snider, "Microwave radiometer facilities at the Wave Propagation Laboratory," in *Proc. NAPEX XI* (JPL Rep. D-4647, Jet Propulsion Lab., Pasadena, CA), 1987, pp. 24-27.

[3] F. T. Ulaby, R. K. Moore, and A. K. Fung, *Microwave Remote Sensing: Active and Passive; Volume 1: Microwave Remote Sensing Fundamentals and Radiometry*. Reading, MA: Addison-Wesley, 1981.

[4] J. W. Waters, "Absorption and emission of microwave radiation by atmospheric gases," in *Methods of Experimental Physics*, vol. 12, M. L. Meeks, Ed., pt. B, *Radio Astronomy*. New York: Academic, 1976, sec. 2.3.

[5] H. J. Liebe, "MPM—an atmospheric millimeter-wave propagation model," *Int. J. Infrared Millimeter Waves*, vol. 10, pp. 631-650, 1989.

[6] S. A. Zhevakin and A. P. Naumov, "On the absorption coefficient of electromagnetic waves by water vapour in the 10 $\mu$-2 cm band," *Izv. VUZ Radiofiz.*, vol. 6, pp. 674-695, 1963.

[7] E. P. Gross, "Shape of collision broadened spectral lines," *Phys. Rev.*, vol. 97, pp. 395-403, 1955.

[8] P. W. Rosenkranz, "Interference coefficients for overlapping oxygen lines in air," *J. Quant. Spectrosc. Radiat. Transfer*, vol. 39, pp. 287-297, 1988.

[9] H. J. Liebe and D. H. Layton, "Millimeter-wave properties of the atmosphere: Laboratory studies and propagation modeling," Nat. Telecom. and Inform. Admin., Boulder, CO, NTIA Rep. 87-24, 1987.

[10] D. Deirmendjian, *Electromagnetic Scattering on Spherical Polydispersions*. New York: Elsevier, 1969.

[11] E. H. Grant, T. J. Buchanan, and H. F. Cook, "Dielectric behavior of water at microwave frequencies," *J. Chem. Phys.*, vol. 26, pp. 156-161, 1957.

[12] D. C. Hogg, F. O. Guiraud, J. B. Snider, M. T. Decker, and E. R. Westwater, "A steerable dual-channel microwave radiometer for measurement of water vapor and liquid in the troposphere," *J. Appl. Meteorol.*, vol. 22, pp. 789-806, 1983.

[13] J. B. Snider, "Radiometric observations of cloud liquid water during FIRE," in *Proc. IGARSS '88 Symp.* (Edinborough, Scotland), 1988, pp. 261-262.

[14] W. L. Smith, H. E. Revercomb, H. B. Howell, H. M. Woolf, R. O. Knuteson, R. G. Dedecker, M. J. Lynch, E. R. Westwater, P. T. May, R. S. Strauch, B. Stankov, and W. A. Dabbert, "GAPEX—A Ground-based Atmospheric Profiling EXperiment," *Bull. Amer. Meteor. Soc.*, vol. 71, pp. 310-318, 1990.

[15] W. E. Hoehne, "Precision of National Weather Service upper air measurements," NOAA Tech. Memo. NWS T & ED-16, [NITS Pub. PB81-108316], 1980.

[16] E. R. Westwater, I. A. Popa Fotino, and M. J. Falls, "Ground-based microwave radiometric observations of precipitable water vapor: a comparison with ground-truth from two radionsonde observing systems," *J. Atmos. Oceanic Tech.*, vol. 6, pp. 724-730, 1989.

[17] E. R. Westwater, "The accuracy of water vapor and cloud liquid determination by dual-frequency ground-based microwave radiometry," *Radio Sci.*, vol. 13, pp. 677-685, 1978.

[18] F. I. Shimabukura and E. E. Epstein, "Attenuation and emission of the atmosphere at 3.3 mm," *IEEE Trans. Antennas Propagat.*, vol. AP-18, pp. 485-490, 1970.

[19] P. Ciotti, E. R. Westwater, M. T. Decker, A.J. Bedard, and B. B. Stankov, "Ground-based microwave radiometric observations of the temporal variation of atmospheric geopotential height and thickness," *IEEE Trans. Geosci. Remote Sensing*, vol. GE-25, pp. 600-615, 1987.

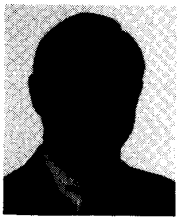

**Ed R. Westwater** received the B.A. degree in physics and mathematics from Western State College of Colorado in 1959, the M.S. degree in physics in 1962, and the Ph.D. degree in physics in 1970 from the University of Colorado.

Since joining the Boulder Laboratories of the U.S. Department of Commerce in 1960, his research has been concerned with microwave absorption in the atmosphere, microwave and infrared radiative transfer, ground- and satellite-based remote sensing by passive radiometry, and in the application of mathematical inversion techniques to problems in remote sensing. He currently serves as Chief of the Thermodynamic Profiling Program Area, Wave Propagation Laboratory, Environmental Research Laboratories, National Oceanic and Atmospheric Administration, Boulder, CO.

Dr. Westwater is the author of 98 publications including technical journal articles, several chapters in books, as well as numerous technical reports, and has been the recipient of two distinguished Authorship Awards by the U.S. Department of Commerce. In addition, he was a member of the ad hoc Working Group on Inversion Methods, Radiation Commission of the International Association of Meteorology and Atmospheric Physics, and was a member of the Committee on Radio Frequencies of the U.S. National Research Council, is a member of URSI/USNC Commission F, a member of the International TOVS Working Group, the International Working Group on InterComparison of Transmittance and Radiance Algorithms sponsored by the Radiation Commission, and is a member of the Working Group on Profiler Systems. In addition to formal publications, he has presented several invited and contributed lectures at various national and international scientific conferences. He was an instructor for three IFORS short courses, "Inversion Methods: Their Applications to Atmospheric Remote Sensing"; CU-NOAA short course: "Remote Sensing of the Troposphere"; and IGARSS '84 Remote Sensing Series "Remote Sensing of the Atmosphere by Microwave Radiometers." He was a Visiting Professor in the Department of Electronics at the University of Rome in 1988 and taught at the Atmospheric Instrumentation Workshop in Taiwan, Republic of China in 1990. His professional memberships include the American Meteorological Society, the Mathematical Association of America, the Society for Industrial and Applied Mathematics, and the American Association for Advancement of Science.

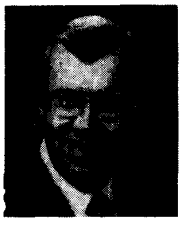

**Jack B. Snider** (M'61-M'66) received the B.S. degree in electrical engineering from the University of Kansas, Lawrence, in 1957 and has continued graduate study at the University of Colorado, Boulder.

From 1957 to 1960 he was employed by the Bendix Corporation. In 1960 he joined the staff of the Central Radio Propagation Laboratory, National Bureau of Standards, where he participated in and directed several research projects in tropospheric radio propagation. He transferred to the Wave Propagation Laboratory (WPL), Environmental Research Laborato-

ries, upon its creation in 1967 where he designed several microwave and millimeter-wave radiometers used in measurement of atmospheric absorption and in remote sensing of the temperature structure of the lower atmosphere. In 1972, he transferred to the Sea State Studies Program Area of WPL where he was concerned with development of experimental techniques for remote measurement of ocean wave characteristics using both surface wave and over-the-horizon high frequency radars. He returned to the Radio Meteorology Program Area (now Thermodynamic Profiling) in 1977. Since then he has been responsible for projects dealing with remote measurement of atmospheric water vapor, liquid water in clouds, temperature profiles, and precipitation. He pioneered the use of microwave radiometry in the observation of supercooled liquid water and has participated in a number of weather modification programs to augment mountain snowpack. His most recent research has been concerned with the relationship between liquid water and the reflectivity of marine stratocumulus clouds. He has authored or contributed to more than 60 scientific papers and technical reports.

Mr. Snider is a member of Tau Beta Pi, Eta Kappa Nu, U.S. Commission F of the International Union for Radio Science (URSI), and the American Geophysical Union.

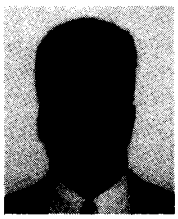

**Michael J. Falls** was born in Pickens, MS, in 1959. He received the B.S. degree in computer science from Jackson State University, Jackson, MS, in 1982.

Since 1981 he has worked at the Wave Propagation Laboratory of the Environmental Research Laboratories, National Oceanic and Atmospheric Administration (NOAA), Boulder, CO, where he has been involved in microwave absorption in the atmosphere, as well as the application of mathematical inversion techniques to problems in remote sensing. He is the author of 17 publications including technical journal articles, a book chapter, and technical reports.